HEFAT2010
7th International Conference on Heat Transfer, Fluid Mechanics and Thermodynamics
19-21 July 2010
Antalya, Turkey

ANALYSIS OF FLOW FIELDS ABOUT GRASS SPECIES (*POACEAE*) USING CFD APPROACH

Krick, J.* and von Lavante, E. and Lahoubi, M. and Cresswell, J.E. and Pennel, C. and Patrick, M.A.
*Author for correspondence
Department of Fluid Mechanics,
University of Duisburg-Essen,
Lotharstraße 1,
47057 Duisburg,
Germany,
E-mail: julian.krick@stud.uni-due.de

ABSTRACT

Grass species from the *Poaceae* family exhibit a large variety of their pollen receiving structures, although, they are pollinated by the same agent – the wind. Biologists assume that different architecture types use different pollen capture mechanisms in order to increase the pollen capture efficiency. In this study the flow about computer models of grass plants with four different architectures was investigated using a CFD approach. The goal was to estimate the relevance of microscopic plant structures on the capture efficiency.

INTRODUCTION

The 'adaptationist programme' of evolutionary biology seeks to explain the form of organisms by demonstrating its functional value. Grass species (*Poaceae*) pose a particular problem for adaptationists, since their architecture is not converging on a single optimal form, although most grasses are pollinated by the wind. Adaptationists argue that different plant architectures function differently while improving the pollen capture efficiency (C%).

Theories about pollen capture mechanisms of grass structures have been concluded from results of field and wind tunnel experiments [1] [2] [3]. For validation of these theories, it is necessary to investigate the microscopic interactions of single pollen grains with individual florets of a flower. This is difficult to realize by wind tunnel or field tests, whereas by means of CFD, a close investigation of the flow details about grass plants seemed feasible [4].

Three questions defined the focus of this study:

1. Does the structure of grass species alter the airflow so that C% is improved?
2. What are the mechanisms of pollen capture?
3. To what extend is CFD able to facilitate and improve the accuracy of investigations on wind pollination mechanisms?

In this study, the air and pollen flow around whole grass plants with four different architectures (diffuse/compact inflorescences with small/large florets) was investigated using CFD. For the determination of C%, a discrete phase of pollen-like particles was released windward to the plant model. The properties of these particles (density/diameter) were varied. Furthermore, several wind speeds and orientations of the plant towards the wind were simulated. The pollen capture mechanisms were investigated by visually sampling trajectories of single particles.

NOMENCLATURE

C%	[-]	Capture Efficiency
v_{set}	[cm s^{-1}]	Settling velocity
ρ	[kg m^{-3}]	Density
g	[m s^{-2}]	Gravitational acceleration
μ	[kg $m^{-1}s^{-1}$]	Volumetric heat generation density
n	[-]	Number of particles
u_{wind}	[m s^{-1}]	Wind speed
l_{ch}	[m]	Characteristic length
Re	[-]	Reynolds number

Abbreviations	
CFD	Computational fluid mechanics
DIC	Direct inertial collision
LeeSed	Leeward sedimentation
IIC	Indirect inertial collision

Subscripts	
mean	Mean value
max	Maximum value
min	Minimum value
wF	With floral structure
nF	Without floral structure
p	Particle
f	Fluid

GRASSES

All grass species, which functioned as templates for the models analysed in this study belong to the family *Poaceae*, whose members are of significant importance to human economy and nourishment.

The flowers or florets of the plants contain male and female reproduction organs, called stigmas and anthers, respectively (compare Figure 1). The stigma has a feather like structure and filters pollen grains out of the airflow. At the bottom of the stigmas there is the ovary. The anthers are slender cylinders attached to long filaments. They are the pollen releasing organs of the flower. Stigmas and anthers are enclosed by two leaves, or bracts (lemma and palea). The group of these elements build up a floret. Groups of florets are arranged in spikelets, which enclose their members by another two bracts (glumes).

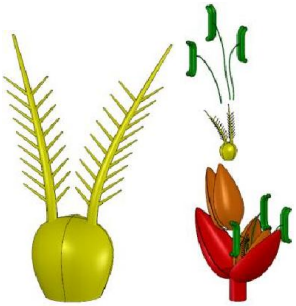

Figure 1 A grass spikelet (red) with floret (orange), stigma with ovary (yellow) and anthers (green)

The structure in which the spikelets are composed around the main axis of the plant is referred to as inflorescence or architecture. The great variety of inflorescence forms can be classified in two binary groups [3], which are depicted in Figure 2. Plants are being distinguished by their small or large spikelets and diffuse or compact inflorescence. In this study, the flow around models of plants from all four classes was simulated.

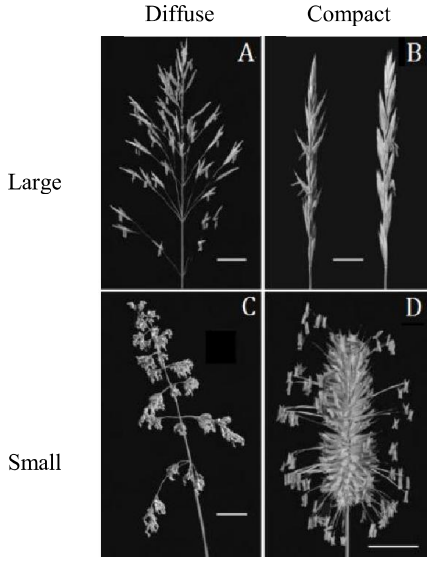

Figure 2 Four morphological classes [3]

THEORY OF POLLEN RECEIPT

Theories of pollen capture mechanisms of grass structures have been concluded from results of field and wind tunnel experiments [1] [2] [3]. In these studies, two principle pollination methods became apparent:

(A) Direct inertial collision (DIC) occurs when pollen grains have enough momentum to diverge from the streamlines of the airflow around an object, penetrate its boundary layer and subsequently impact on the plant's surface. The main physical properties which affect this capture mode are the momentum of the particle and the boundary layer, including the deflection of streamlines.

(B) Leeward Sedimentation (LeeSed): pollen captured is theoretically possible by a process of LeeSed in which pollen grains pass the plant structure, but get entrained into downstream separation vortices, created by the flower. Subsequently, they recirculate behind the plant and may be transported back towards the receptive stigmas [1] [2].

SETTLING VELOCITY

The settling velocity (v_{set}) is the rate of fall of small, spherical particles in still air. This measure is commonly used to define the aerodynamic properties of pollen grains [5]. It can be calculated using Stoke's law:

$$v_{set} = \frac{2(\rho_p - \rho_f) g r^2}{9\mu}$$

where v_{set} is the settling velocity in [cm s^{-1}], ρ_p and ρ_f are the pollen and fluid density in [kg cm^{-3}], r being the radius of the pollen grain in [cm], g is the gravity in [cm s^{-2}] and μ is the fluid's dynamic viscosity in [kg cm^{-1} s^{-1}].

CAPTURE EFFICIENCY

The capture efficiency C% is a measure for the pollination performance of a plant. It is defined as the ratio of the number pollen grains captured by the female receptor (the stigmas) n_{wF} to those which would have been blown through the cross-sectional area of the female receptors, had the plant not been present in the airstream n_{nF} [6]. Thus,

$$C\% = \frac{n_{wF}}{n_{nF}}$$

COMPUTER MODELS AND SIMULATIONS

For the simulations of flow around whole plant structures, four different computer models have been created (Figure 3), using GAMBIT® (Fluent Inc., Lebanon, New Hampshire, USA). Each model represents one member of the four morphological classes, in Figure 2. The dimensions of these models are based on measurements of floral and inflorescence characteristics for grass species published in [3]. The

geometries were intended to be generic and not to fit a specific species.

In the compact cases, the flowers were simulated at turning angles of 0°, 45° and 90° around their vertical axis, in order to study the dependency of C% on the orientation. The diffuse inflorescences were oriented at angles of 0° and 45° around a horizontal axis. The spikelets of the diffuse models did not show a preferred orientation, thus the model was not turned around its vertical axis. Furthermore, wind speeds at u_{wind} = 0.5, 1, 3 m s^{-1} were examined.

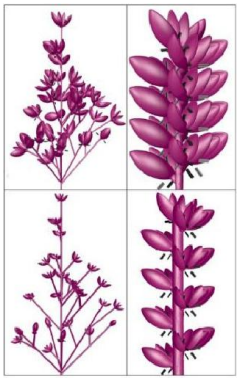

Figure 3 Computer models of generic grass plants with stigma planes (black)

Each spikelet possesses five sets of two perpendicular stigma planes radiating from the ovary (Figure 4). They were arranged in such a way, that they match the position of stigmas for natural plants. The stigma planes did capture the released particles.

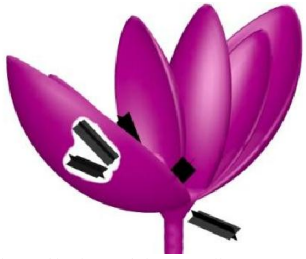

Figure 4 Single spikelet with two florets and stigma planes (black)

The simulated fluid was air at a temperature of T = 288.16 K and an atmospheric pressure of p = 101.325 kPa. Its density and dynamic viscosity were set to ρ = 1.225 kg m^{-3} and μ = 1.7894 kg m^{-1} s^{-1}, respectively. FLUENT® (Fluent Inc. Lebanon, New Hampshire, USA) version 6.2 software was employed as a solver and post-processor.

The domain around the models was cuboid, and consisted of one inlet, defined as 'velocity inlet', and one outlet, defined as 'outflow'. Both patches were opposite to each other, in front of and rearward to the plant geometry. The four sides of the domain were 'moving walls' translating at the same velocity as the airflow at the inlet. The plant surfaces were assigned with the 'wall' boundary condition, whereby the collisions of particles and plant surface were modelled as completely elastic. The particle trapping elements, the stigma plane, were assigned with a special boundary condition, which did not alter the fluid or particle flow. However, if a particle moved through the area of a stigma plane, it was trapped and counted.

For the determination of the Reynolds number, two different characteristic lengths (l_{ch}) were used. For the compact models l_{ch} was defined to be the inflorescence width, since compact inflorescences act as single bodies [1]. With l_{ch} = $11.2 \cdot 10^{-3}$ m for the widest compact inflorescence, the maximum Reynolds number results in Re = $2.3 \cdot 10^{3}$. For diffuse architectures l_{ch} was chosen to be the length of a single spikelet, since spikelets in diffuse inflorescences alter airflow independently [1]. The longest spikelet has a length of l_{ch} = $21.69 \cdot 10^{-3}$ m, so that the Reynolds number results in Re = $4.5 \cdot 10^{3}$.

These Reynolds numbers are smaller than Re_{crit}= $5 \cdot 10^{5}$, which is the critical Reynolds number for flow over a flat plate [7]. For this reason a laminar flow model had been chosen to simulate viscous effects . The flow was assumed to be steady as well as incompressible (Ma << 0.3), which is why a segregated, implicit solver has been employed. The governing equations were discretized implementing first order accuracy. The solver performed calculations in single precision mode. Furthermore, pressure and velocity were coupled by the SIMPLE algorithm. The influence of gravity on the particles was neglected.

For the simulation of pollen in FLUENT©, a discrete phase model was used, i.e. 32500 spherical particles were released at the inlet of the domain, covering the cross section of the whole plant model. These particles were varied in diameter and density, in order to simulate various pollen types. Since it is more common to characterize pollen particles by diameter and settling velocity, these two properties are used in the following. The values of diameter and settling velocities were adopted from [2] [3] and [6]. The densities of particles (necessary for definition of discrete phase in FLUENT©) were calculated from the settling velocity and the diameter using Stoke's law. Due to time reason, only a single pollen diameter of 30 microns has been selected. The settling velocities were chosen to be 2, 5 and 10 cm s^{-1}, which refers to densities of 112.2, 1278.1 and 3649.3 kg m^{-3}. Table 1 summarizes all simulated plant and pollen parameters.

Table 1 Summary of all simulation parameters

Inflorescence Architectures	Spikelets Sizes	Orientations	
Compact	Large	for compact:	0°
			45°
			90°
Diffuse	Small	for diffuse:	0°
			45°
Wind Speeds	**Settling Velocities**	**Densities**	**Pollen Diameter**
0.5	2	112.2	
1	5	1278.1	30
3	10	3649.3	

MEASUREMENTS

Two types of measurements have been performed. Initially, the trajectories of 4 to 17% of the captured pollen particles for one simulation were examined, in order to determine if and to what extend particles were trapped due to LeeSed. This information was essential for the analysis of the results. The

trajectories were categorised into three different groups. The first group corresponded to capture by sedimentation. The second group included particles which were trapped by DIC. In this case the particles directly hit the stigma planes. A third group corresponded to those particles which hit the plant structure at least once before captured by a stigma plane (Figure 5). In the following, this capture mode is named as indirect inertial collision (IIC).

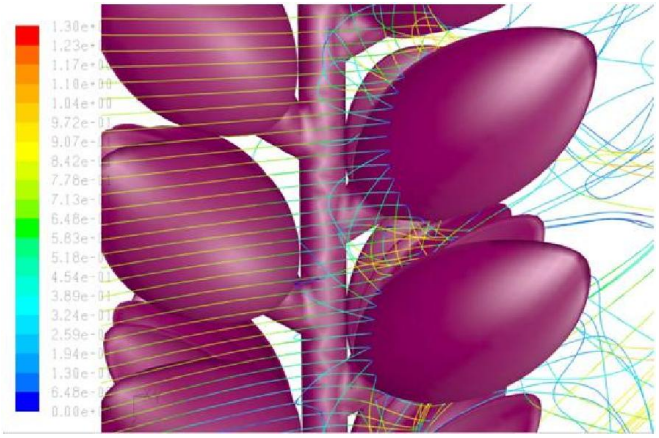

Figure 5 Collisions of particles with plant

In the second group, the capture efficiency for each case has been determined. Therefore, two simulations for each case had to be performed. In one simulation, the plant structure was present and did alter the airflow, as well as the trajectories of particles. Here n_{wF} was determined. In the second simulation, only the stigma planes were present. The planes themselves did not alter the air or particle flow, thus being the ideal stigmas. The number of captured particles in these simulations corresponds to n_{nF}.

RESULTS

The evaluation of the pressure and velocity fields around the current geometries was not included in this section. Both fields were found to be according to expectations based on common fluid mechanic experiences.

For the single cases abbreviations are introduced: the expression CL45°-3ms^{-1}-2cms^{-1} specifies a compact inflorescence with large spikelets at an orientation of 45°, a wind speed of 3 m s^{-1} and a settling velocity of the injected particles of 2 cm s^{-1}.

Trajectory Sampling

The results of the examination of particle trajectories (Table 2 Results for the pollen trajectory sampling) indicate that particles do recirculate in leeward eddies (Figure 6), but pollen capture by sedimentation is rare. In three of the analyses cases, 1 out of 50 particles has been trapped by recirculation. Most particles were captured by DIC or IIC.

Capture Efficiency

The common mean capture efficiency calculated over all analyzed cases results in 61% ± 18.54% (mean ± SD). The overall maximum and minimum values are 126.60% and 27.20% for the simulations of CL0° and CS45°, respectively. In 6.67% of all calculations the plant structure had a positive effect on pollination, i.e. C% > 100%. Five of these cases occurred for CL0°, one of them for CS0°. In the major part of the simulations the pollination efficiency increases with wind speed and pollen density (i.e. settling velocity).

Figure 6 Trajectories of recirculating particles

Table 2 Results for the pollen trajectory sampling

Settling Velocity: 5, No. of trajectories sampled: 50				Settling Velocity: 2, No. of trajectories sampled: 50			
Wind Speed: 0.5		Wind Speed: 1.0		Wind Speed: 0.5		Wind Speed: 1.0	
CL45°		CL45°		CL45°		CL45°	
sedimentation	0	sedimentation	0	sedimentation	1	sedimentation	1
DIC	23	DIC	14	DIC	34	DIC	36
IIC	27	IIC	36	IIC	15	IIC	13
CS45°		CS45°		CS45°		CS45°	
sedimentation	0	sedimentation	1	sedimentation	0	sedimentation	0
DIC	20	DIC	22	DIC	40	DIC	42
IIC	30	IIC	27	IIC	10	IIC	8

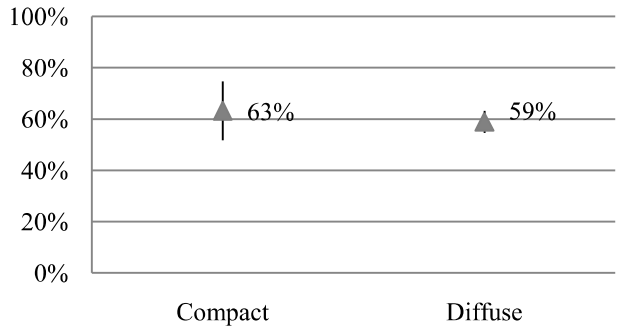

Figure 7 Mean ± SD for both inflorescence types; C% vs. inflorescence architecture

Figure 7 illustrates, that the mean values of C% for compact and diffuse inflorescences are 63% ± 22.81% (range = 99.40%, max. = 126.60%, min. = 27.2%) and 58% ± 8.65% (range = 29.28%, max. = 85.12%, min = 41.32%), respectively. Thus, over a large range of orientations, wind speeds, pollen densities and floret sizes the capture efficiencies for both types of inflorescences are quiet similar. However, the spectrum of C%-

values for compact architectures is larger than for diffuse ones, as the difference in the standard deviations indicates.

Thus, the diffuse structure stabilises a nearly constant capture efficiency of intermediate amplitude while the influences factors change. In contrast to that, C% for compact plant structures varies largely with changes in the influencing variables. It reaches significantly higher and lower C%-values than the diffuse type does.

When we regard the compact inflorescences, the mean C% differs depending on the spikelet size of the flower. This effect can be observed in both inflorescence types, however with a contrary behaviour. As Figure 8 shows, $C\%_{mean}$ (66%) for CL is larger than for CS (60%), however the difference is rather small. Unlike in the compact case, $C\%_{mean}$ (55%) for DL is smaller than for DS (61%), but also very similar. The maximum capture efficiencies for the compact inflorescences are 126.60% and 102.60% for CL and CS, respectively. There is a larger difference in these figures, in comparison to the compact's minimum values (CL: $C\%_{min}$ = 29.15%, CS: $C\%_{min}$ = 27.20%).

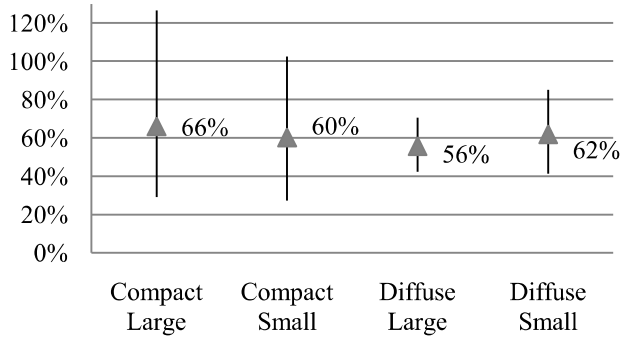

Figure 8 Mean, Max. and Min. C% for both Inflorescence Types and Spikelet Sizes; C% vs. Inflorescence Architecture and Spikelet Size

Thus, one can say that CL reaches more often higher C%-values than CS, whereas there are no major differences in the minimums. The diffuse inflorescences show also this kind of behaviour. The minimum C%-values are quiet similar (DL: $C\%_{min}$ = 42.32%; DS: $C\%_{min}$ = 41.32%), whereas the difference between the maximum deflections of the capture efficiencies are rather large (DL: $C\%_{max}$ = 70.60%; DS: $C\%_{max}$ = 85.12%).

Generally, as mentioned above, C% increases with wind speed and pollen density.

CONCLUSION

The results of the pollen trajectory sampling disprove the assumption that capture by LeeSed is a major mechanism in pollination. They rather show that most particles were captured by DIC. Another significant capture mode in the simulation was capture by IIC, however, whether or not this effect will also appear in natural environments is not clear, because the collision between particles and plant structure were fully elastic and thus not analogous to reality. Furthermore, gravity was not considered, so that particles did not sink to the ground while colliding with the plant.

Generally, the results of this study confirm the assumption that the shape of the compact and diffuse inflorescences was adapted to enhance pollination. The compact architectures can even reach capture efficiencies larger than 100%. By contrast, the performance of the diffuse models rarely went beyond 80%, but was more constant. However, over a wide spectrum of parameters (i.e., wind speeds, orientations, pollen density.), both architectures have, at least in idealized conditions, similar mean pollination efficiencies. This suggests that different inflorescence types may have adapted their geometry to optimize pollination success under a range of environmental conditions.

Overall, the results of this study seem reasonable and largely confirm previous pollination theory. However, the application of the results to other experiments or even natural environments must be done with caution, because in the present simulations several (unnatural) models have been applied, such as steady, laminar flow and non-oscillating geometry. These models render the natural behaviour of the flow and the plant in an idealised approach. The influence of idealisations on the results cannot be estimated unless further studies investigate them. However, the simulations show that CFD is able to support the microscopic analysis of pollination mechanisms in addition to wind tunnel and field experiments.

A major task for further CFD investigations of pollination mechanisms would be the development of a method by which the quantity of pollen capture by sedimentation can be determined more precisely and faster than by manually sampling a certain number of particle trajectories. Furthermore, investigations on the collision behavior of pollen particles and plants are necessary in order to simulate the bouncing-effect more accurately. The results of this study showed that capture by indirect inertial collision is a major capture mode. Therefore, a proper emulation of collision characteristics could produce more realistic capture efficiencies. One way to do this is to determine the coefficient of restitution for a collision between a pollen grain and a plant surface.

REFERENCES

[1] Niklas, K.J., The aerodynamics of wind pollination, *Botanical Review,* Vol. 51, 1985, pp. 328-386

[2] Friedman, J. and Harder, L.D., Inflorescence architecture and wind pollination in six grass species, *Functional Ecology,* Vol. 18, 2004, pp. 851-860

[3] Friedman, J. and Harder, L.D., Functional associations of floret and inflorescence, *American Journal of Botany,* Vol. 92, 2005, pp. 1862-1870

[4] Cresswell, J.E. and Henning, K. and Pennel, C. and Lahoubi, M. and Patrick, M.A. and Young, P.G. and Tabor, G.R., Conifer ovulate cones accumulate pollen principally by simple impaction, *Proceedings of the National Academy of Sciences of the United States of America*, Vol. 104, 2007, pp. 18141-18144.

[5] Di-Giovanni, F. and Kevan, P.G. and Nasr, M.E., The variability in settling velocities of some pollen spores, *Grana*, Vol. 34, 1995, pp. 39-44

[6] Paw U., K.T. and Hotton, Optimum pollen and female receptor size for anemophily, *American Journal of Botany*, Vol. 76, 1989, pp. 445-453

[7] Schlichting, H. and Gersten, K. and Krause, E. and Oertel Jr., H., Grenzschicht-Theorie, 10th edition, *Springer*, 2006